UNIVERSAL WISER
PUBLISHER

Research Article

Fractional-Order Modeling and Stability Analysis of HIV Infection with and Without Antiretroviral Therapy Treatment

Hicham Saber[1], Khaled Aldwoah[2]*[iD], Abdelkader Moumen[1][iD], Sabri T. M. Thabet[3,4]*[iD], Tariq A. Alraqad[1], Alaa M. Abd El-latif[5], Etaf Alshawarbeh[1]

[1] Department of Mathematics, College of Science, University of Hail, Hail, 55473, Saudi Arabia
[2] Department of Mathematics, Faculty of Science, Islamic University of Madinah, Madinah, 42351, Saudi Arabia
[3] Department of Mathematics, Saveetha School of Engineering, Saveetha Institute of Medical and Technical Sciences, Saveetha University, Chennai, Tamil Nadu, 602105, India
[4] Department of Mathematics, College of Science, Korea University, 145 Anam-ro, Seongbuk-gu, Seoul, 02814, Republic of Korea
[5] Mathematics Department, College of Science, Northern Border University, Arar, 91431, Saudi Arabia
 E-mail: aldwoah@iu.edu.sa; th.sabri@yahoo.com

Abstract: This article formulates and examines a fractional-order model for Human Immunodeficiency Virus (HIV) infection using Caputo's derivative in order to model memory-reliant dynamics. The model describes interactions among uninfected, infected, and latently infected CD4$^+$ T cells and between free virus particles with and without the effect of Antiretroviral Therapy (ART). We derive major theoretical results of positivity, boundedness, existence, and uniqueness of solutions based on fixed-point theory and fractional calculus. Additionally, we perform a Picard stability analysis, which involves constructing a sequence of successive approximations and proving that small perturbations in initial data lead to proportionally small changes in the solution. We numerically solve the model using Lubich's convolution quadrature method to simulate its behavior across various fractional orders and ART scenarios. The findings indicate that fractional dynamics are in closer agreement with the chronic characteristics of HIV infection and that ART efficacy increases as a function of increasing order of fractionality, which implies lesser memory effects and faster immune response.

1. Introduction

Fractional calculus, which generalizes classical differentiation and integration to non-integer orders, has emerged as a powerful tool in modeling memory-dependent systems. Its non-local nature enables better representation of biological processes that depend not only on the current state but also on historical states. In recent years, Fractional Differential Equations (FDEs) have been increasingly applied to epidemiology and immunology, offering improved realism over classical integer-order models [1–4].

The use of FDEs in infectious disease modeling has led to more accurate representations of disease progression, latency, and immune memory. Applications include models of tuberculosis, hepatitis, dengue, and Corona Virus Disease (COVID-19), where memory effects play a role in viral replication, immune response, and therapeutic delay [5, 6]. The fractional-order parameter allows for continuous tuning between short-term and long-term memory responses, enhancing model flexibility and data fitting capabilities.

Mathematical modeling has been an essential tool for understanding the transmission and progression of infectious diseases [7, 8]. Traditional models based on systems of Ordinary Differential Equations (ODEs) have been useful in elucidating disease spread dynamics for acute infections. However, these models are generally inadequate in describing biological processes that exhibit memory and hereditary properties [9]. To address these shortcomings, researchers have increasingly employed fractional calculus [10, 11]. In biology, it plays an important role in simulating different infectious diseases, such as Ebola Dynamics [12], breast cancer [13, 14], and Liver Fibrosis Disease [15].

The application of fractional differential equations, especially those involving Caputo-type derivatives, has become increasingly prominent in diverse scientific disciplines, ranging from viscoelasticity and control theory to signal processing and, more recently, epidemiology [16, 17]. Within infectious disease modeling frameworks, fractional-order models have been shown to successfully capture delayed immune responses, sub-diffusive transport, and persistent infections that are not adequately described by conventional ODEs [18]. These models are particularly suitable for analyzing diseases characterized by long incubation periods or chronic behavior.

Human Immunodeficiency Virus (HIV) is one such disease, marked by an extended latent period, immune system deterioration, and complex within-host dynamics. $CD4^+$ T lymphocytes are primarily targeted by the virus, resulting in a gradual decline in these cells and eventual progression toward Acquired Immunodeficiency Syndrome (AIDS) if left untreated. Traditional models of HIV infection have provided valuable insights into viral replication, immune system interactions, and treatment efficacy [19, 20], but they rarely account for memory-like immune responses and latent infection reservoirs. In contrast, several recent studies based on vector-host formulations have explored broader transmission dynamics, offering additional perspectives on the long-term behavior of infection [21–23]. Moreover, while it is widely documented that Antiretroviral Therapy (ART) helps reduce viral loads and prolong patient survival, limited effort has been made to assess the effect of ART within a fractional-order framework that incorporates memory effects [24]. The authors in [25] proposed the following model for HIV infection as:

$$\frac{d}{dt}X(t) = \Lambda + \frac{r}{\kappa + V(t)}X(t)V(t) - \mu X(t)V(t) - \delta_1 X(t),$$

$$\frac{d}{dt}Y(t) = \gamma\mu X(t)V(t) + \sigma Z(t) - \delta_2 Y(t),$$

$$\frac{d}{dt}Z(t) = (1-\gamma)\mu X(t)V(t) - \sigma Z(t) - \delta_3 Z(t),$$

$$\frac{d}{dt}V(t) = \xi Y(t) - \delta_4 V(t),$$

(1)

where $X(t)$ represents uninfected $CD4^+$ T cells, $Y(t)$ denotes actively infected $CD4^+$ T cells, $Z(t)$ represents latently infected $CD4^+$ T cells, and $V(t)$ denotes the concentration of viruses.

ART-modified system. ART reduces (i) infection of healthy $CD4^+$ T cells by free virus and (ii) production of new virions from productively infected cells. We represent these effects by efficacies ε_I, $\varepsilon_P \in [0, 1]$ applied to the infection and production rates, optionally modulated by adherence $u(t) \in [0, 1]$:

$$\mu_{\text{ART}}(t) = \left(1 - \varepsilon_I u(t)\right)\mu, \quad \xi_{\text{ART}}(t) = \left(1 - \varepsilon_P u(t)\right)\xi.$$

Replacing μ and ξ in (1) gives the ART system

$$^{C}D_t^{\theta} X(t) = \Lambda + \frac{rX(t)V(t)}{\kappa + V(t)} - \mu_{\text{ART}}(t)X(t)V(t) - \delta_1 X(t),$$

$$^{C}D_t^{\theta} Y(t) = \mu_{\text{ART}}(t)X(t)V(t) - \delta_2 Y(t) + \sigma Z(t),$$

$$^{C}D_t^{\theta} Z(t) = (1 - \gamma)\mu_{\text{ART}}(t)X(t)V(t) - \delta_3 Z(t) - \sigma Z(t),$$

$$^{C}D_t^{\theta} V(t) = \xi_{\text{ART}}(t)Y(t) - \delta_4 V(t).$$

(2)

ART is assumed to reduce both the infection of healthy CD4$^+$ T cells by free virus and the production of new virions from infected cells. Let $t_{\text{ART}} = 5$ days be the treatment initiation time, and let $\varepsilon_\mu,\ \varepsilon_\xi \in [0,\ 1]$ denote the corresponding drug efficacies. We define

$$\mu_{\text{ART}} = \begin{cases} \mu, & t < t_{\text{ART}}, \\ (1 - \varepsilon_\mu)\mu, & t \geq t_{\text{ART}}, \end{cases} \qquad \xi_{\text{ART}} = \begin{cases} \xi, & t < t_{\text{ART}}, \\ (1 - \varepsilon_\xi)\xi, & t \geq t_{\text{ART}}. \end{cases}$$

Thus, the infection rate and virion production rate decrease by 80% and 70%, respectively, after therapy initiation. The other parameters remain unchanged.

In this study, we formulate and examine a fractional-order HIV infection model using Caputo derivatives of order $\theta \in (0,\ 1]$. The model describes interactions between uninfected CD4$^+$ T cells, actively infected cells, latently infected cells, and free virus particles. We explore two scenarios: with and without antiretroviral therapy, which is incorporated by modifying infection, replication, and clearance-related parameters. Our aim is to investigate the effects of memory-dependent dynamics, governed by the fractional order θ, on disease progression and treatment effectiveness.

1.1 *Motivation for the fractional-order model*

Classical HIV models typically rely on integer-order differential equations, assuming that the rate of change of system states depends only on their current values. However, biological processes, particularly those involving immune response and virus-host interactions, often exhibit memory and hereditary characteristics.

Fractional calculus provides a natural extension to classical models by incorporating memory effects through non-local operators. In particular, Caputo fractional derivatives allow for the inclusion of past states of the system, weighted by a power-law kernel, captures long-term memory more accurately. This is especially relevant in HIV dynamics, where immune memory, latency periods, and delayed responses to treatment are critical.

Therefore, transitioning from an integer-order to a fractional-order formulation enables a more realistic description of the progression and control of HIV infection, and has been supported in recent literature on infectious disease modeling [26, 27].

To better capture these memory-dependent processes, we generalize the system using Caputo fractional derivatives of order $\theta \in (0, 1)$, resulting in the fractional-order system. The fractional-order HIV model using Caputo derivatives of order $\theta \in (0, 1]$ can be expressed as:

$$^{C}D_t^{\theta}X(t) = \Lambda + \frac{r}{\kappa + V(t)}X(t)V(t) - \mu X(t)V(t) - \delta_1 X(t),$$

$$^{C}D_t^{\theta}Y(t) = \gamma \mu X(t)V(t) + \sigma Z(t) - \delta_2 Y(t),$$

(3)

$$^{C}D_t^{\theta}Z(t) = (1 - \gamma)\mu X(t)V(t) - \sigma Z(t) - \delta_3 Z(t),$$

$$^{C}D_t^{\theta}V(t) = \xi Y(t) - \delta_4 V(t),$$

with initial conditions:

$$X(0) = X_0 > 0, \quad Y(0) = Y_0 > 0, \quad Z(0) = Z_0 > 0, \quad V(0) = V_0 > 0,$$

and parameters Λ, r, κ, μ, δ_1, δ_2, δ_3, δ_4, ξ, γ, σ are positive constants. The fractional derivative $^{C}D_t^{\theta}$ is defined in the Caputo sense with order $\theta \in (0, 1]$.

The main contributions of this work are as follows:

• We extend the existing within-host HIV model (1) by incorporating fractional-order dynamics to capture the long-term memory effects of immune response and viral persistence.

• We rigorously analyze the theoretical foundations of the model, proving the well-posedness and stability of the fractional system.

• We provide numerical solutions using a robust and convergent method [28], allowing for realistic simulations under varying fractional orders and treatment conditions.

• We demonstrate that ART effectiveness increases with the fractional order, suggesting a strong interplay between memory effects and treatment response.

By integrating theoretical analysis, stability considerations, and numerical simulations, our work presents a comprehensive framework for understanding HIV dynamics within a fractional-order context. This approach not only enhances the biological realism of existing models but also opens new avenues for more nuanced investigations into treatment strategies for chronic infectious diseases.

The remainder of this paper is structured as follows. In Section 2, some basic definitions are provided. In Section 3, we establish theoretical and numerical characteristics and analysis of the model, including positivity and boundedness, fixed-point theory and Picard iteration, etc. Section 4 provides graphical analysis and interpretation of simulation results across different fractional orders and ART scenarios. Section 5 concludes with a summary of the findings and their biological implications.

2. Preliminaries on fractional calculus

Fractional calculus generalizes classical differentiation and integration to non-integer (real or complex) orders. For $0 < \theta \le 1$, the most commonly used definitions are as follows:

Definition 1 [29] (Liouville fractional integral) Let $f(t)$ be a continuous function on $[0, T]$. The Riemann-Liouville fractional integral of order $\theta > 0$ is defined by

$$I^\theta f(t) = \frac{1}{\Gamma(\theta)} \int_0^t (t-\tau)^{\theta-1} f(\tau)\, d\tau,$$

where $\Gamma(\cdot)$ denotes the Gamma function.

Definition 2 [29] (Caputo fractional derivative) Let $f(t)$ be sufficiently smooth. The Caputo fractional derivative of order $0 < \theta \le 1$ is defined as

$$^C D_t^\theta f(t) = \frac{1}{\Gamma(1-\theta)} \int_0^t (t-\tau)^{-\theta} f'(\tau)\, d\tau.$$

The Caputo derivative is particularly suitable for initial value problems in physical and biological systems because it allows for classical initial conditions, such as $f(0) = f_0$.

3. Theoretical and numerical results

Theorem 1 (Positivity and boundedness of the Caputo fractional-order HIV model) Under non-negative initial conditions, the solution $(X(t),\, Y(t),\, Z(t),\, V(t))$ of the Caputo fractional HIV model is:

(i) Positive for all $t > 0$,

(ii) If $\delta_2 > \xi/\delta_4$ (see Lemma 3.1), then the solution of system (3) is uniformly bounded on any finite interval $[0,\, T]$, $T > 0$. This condition represents that infected cells die faster than the virus can be effectively produced, ensuring that all model variables remain bounded for all time.

Remark For the Caputo fractional derivative, positivity is interpreted via its equivalent Volterra integral form rather than a pointwise differential condition. If $^C D_t^\theta y(t) = f(t,\, Y(t))$ with $0 < \theta \le 1$, then

$$y(t) = y(0) + \frac{1}{\Gamma(\theta)} \int_0^t (t-s)^{\theta-1} f(s,\, y(s))\, ds.$$

When $y(0) \ge 0$ and $f(s,\, y) \ge 0$ for $y \ge 0$, the integral remains nonnegative, implying $y(t) \ge 0$ for all $t > 0$. Thus, assuming the right-hand side is nonnegative on the boundary is sufficient to ensure positivity for the Caputo system.

Proof. (i): Positivity

Let $(X(t),\, Y(t),\, Z(t),\, V(t))$ be a solution to the fractional-order HIV model defined in equation (2), with non-negative initial conditions:

$$X(0) = X_0 > 0, \quad Y(0) = Y_0 > 0, \quad Z(0) = Z_0 > 0, \quad V(0) = V_0 > 0.$$

We apply the positivity theorem for Caputo fractional differential equations, which states that if the right-hand side of a system is non-negative on the boundary of the positive orthant, then the solution remains non-negative for all $t > 0$.

We examine each equation when the corresponding state variable is zero, while others remain positive:

• For $X(t) = 0$, we have:

$$^C D_t^\theta X(t) = \Lambda > 0.$$

• For $Y(t) = 0$, since $X, V, Z > 0$, we obtain:

$$^C D_t^\theta Y(t) = \gamma \mu XV + \sigma Z > 0.$$

• For $Z(t) = 0$, using $X, V > 0$, we get:

$$^C D_t^\theta Z(t) = (1 - \gamma)\mu XV > 0.$$

• For $V(t) = 0$, since $Y > 0$, we obtain:

$$^C D_t^\theta V(t) = \xi Y > 0.$$

In each case, the Caputo derivative is strictly positive on the boundary of the positive orthant, which implies that the solution trajectory is directed into the interior of the positive domain. By the standard positivity theorem, all state variables remain positive for all $t > 0$.

(ii) Define the Lyapunov-like function:

$$W(t) = X(t) + Y(t) + Z(t) + \frac{1}{\delta_4} V(t).$$

Using the linearity of Caputo derivatives for sufficiently smooth functions, we compute:

$$^C D_t^\theta W(t) = {}^C D_t^\theta X(t) + {}^C D_t^\theta Y(t) + {}^C D_t^\theta Z(t) + \frac{1}{\delta_4} {}^C D_t^\theta V(t).$$

Substituting the system:

$$^C D_t^\theta W(t) = \Lambda + \frac{rX(t)V(t)}{\kappa + V(t)} - \mu X(t)V(t) - \delta_1 X(t)$$

$$+ \gamma \mu X(t)V(t) + \sigma Z(t) - \delta_2 Y(t)$$

$$+ (1 - \gamma)\mu X(t)V(t) - \sigma Z(t) - \delta_3 Z(t)$$

$$+ \frac{1}{\delta_4}(\xi Y(t) - \delta_4 V(t)).$$

Simplifying:

$$^C D_t^\theta W(t) = \Lambda + \frac{rX(t)V(t)}{\kappa + V(t)} - \delta_1 X(t) - \delta_2 Y(t) - \delta_3 Z(t) + \frac{\xi}{\delta_4} Y(t) - V(t).$$

Using the inequality $\dfrac{rX(t)V(t)}{\kappa + V(t)} \le rX(t)$, we get:

$$^C D_t^\theta W(t) \le \Lambda + rX(t) - \delta_1 X(t) - \left(\delta_2 - \frac{\xi}{\delta_4} \right) Y(t) - \delta_3 Z(t) - V(t).$$

Since $V(t) \ge 0$ and $\kappa > 0$, we have

$$0 \le \frac{V(t)}{\kappa + V(t)} \le 1.$$

Multiplying both sides by $rX(t)$ gives

$$\frac{rX(t)V(t)}{\kappa + V(t)} \le rX(t),$$

which establishes the inequality used in the boundedness proof. This relation expresses the saturating nature of the proliferation term, where the effective proliferation rate cannot exceed r. If $\delta_2 > \dfrac{\xi}{\delta_4}$, then all coefficients of the variables are negative for sufficiently large $W(t)$. Thus, there exists a constant $M > 0$ such that:

$$W(t) > M \quad \Rightarrow \quad {}^C D_t^\theta W(t) < 0.$$

Therefore, $W(t)$ is ultimately decreasing and hence uniformly bounded for all $t > 0$. Since $W(t)$ is a linear combination of the state variables with positive coefficients, all components $X(t)$, $Y(t)$, $Z(t)$, $V(t)$ are also bounded.

Lemma 3.1 (Boundedness condition for infected and viral populations) Let $0 < \theta \le 1$ and suppose $\delta_2 > \xi/\delta_4$. Then there exists a constant $C > 0$ such that

$$Y(t) + \frac{1}{\delta_4} V(t) \le C, \quad t \in [0, T].$$

Proof sketch From the system equations,

$$^C D_t^\theta \left(Y + \frac{1}{\delta_4} V \right) = \gamma \mu XV + \sigma Z - \delta_2 Y + \frac{1}{\delta_4} (\xi Y - \delta_4 V) \le \left(\frac{\xi}{\delta_4} - \delta_2 \right) Y \le 0,$$

where we have neglected the nonnegative terms $\gamma \mu XV$ and σZ. Hence, $Y(t) + \delta_4^{-1} V(t)$ is nonincreasing, and by the fractional comparison principle,

$$Y(t) + \frac{1}{\delta_4}V(t) \le Y(0) + \frac{1}{\delta_4}V(0) =: C. \tag{$\square$}$$

Biological interpretation. The condition $\delta_2 > \xi/\delta_4$ expresses that the rate of loss of infected cells (average lifespan $1/\delta_2$) exceeds the effective viral production per infected cell (ξ/δ_4). Biologically, infected cells die faster than the virus can replenish itself, keeping the infection and virus populations bounded. If the inequality fails, $Y(t)$ and $V(t)$ may grow without bound, indicating uncontrolled viral replication.

Remark 1 In the integer-order case ($\theta = 1$), this same inequality ensures exponential decay of Y and V; for $0 < \theta < 1$, decay is slower but still monotone due to the fractional-memory effect.

Remark 2 The condition $\delta_2 > \dfrac{\xi}{\delta_4}$ ensures that the composite Lyapunov-like function $W(t) = X(t) + Y(t) + Z(t) + \dfrac{1}{\delta_4}V(t)$ is ultimately decreasing, which guarantees boundedness of all state variables. If $\delta_2 \le \dfrac{\xi}{\delta_4}$, the coefficient of $Y(t)$ in $^CD_t^\theta W(t)$ may become nonnegative, and the dissipativity of the system is no longer analytically guaranteed. In such cases, the trajectories may display non-decaying or oscillatory behavior depending on parameter values. Nevertheless, numerical simulations indicate that for parameter values near the equality boundary $\delta_2 = \xi/\delta_4$, the solutions remain biologically feasible (positive and bounded) over finite time horizons, suggesting conditional stability in practical scenarios.

Remark 3 Positivity and boundedness arguments remain valid for the model with ART intervention, because ART only decreases the infection/production terms; the proofs above apply verbatim with $\mu \mapsto \mu_{\text{ART}}(t)$ and $\xi \mapsto \xi_{\text{ART}}(t)$. For constant adherence $u(t) \equiv u^*$, $\mu_{\text{ART}} = (1 - \varepsilon_I u^*)\mu$ and $\xi_{\text{ART}} = (1 - \varepsilon_P u^*)\xi$.

3.1 *Existence and uniqueness of solutions for the caputo fractional-order HIV model*

Consider the initial value problem:

$$^CD_t^\theta \mathscr{Y}(t) = \mathscr{F}(t, \mathscr{Y}(t)), \quad \mathscr{Y}(0) = \mathscr{Y}_0 \in \mathbb{R}^4, \quad 0 < \theta \le 1,$$

where $\mathscr{F} : [0, T] \times \mathbb{R}^4 \to \mathbb{R}^4$ is given, and the Caputo derivative is of order $\theta \in (0, 1]$. Here,

$$\mathscr{Y}(t) = \begin{bmatrix} X(t) \\ Y(t) \\ Z(t) \\ V(t) \end{bmatrix},$$

and the nonlinear right-hand side:

$$\mathscr{F}(t, \mathscr{Y}(t)) = \begin{bmatrix} \Lambda + \dfrac{rX(t)V(t)}{\kappa + V(t)} - \mu X(t)V(t) - \delta_1 X(t) \\ \gamma\mu X(t)V(t) + \sigma Z(t) - \delta_2 Y(t) \\ (1 - \gamma)\mu X(t)V(t) - \sigma Z(t) - \delta_3 Z(t) \\ \xi Y(t) - \delta_4 V(t) \end{bmatrix}.$$

Lemma 3.2 The function $\mathscr{F}(t, \mathscr{Y})$ satisfies:
(i) Joint continuity in $(t, \mathscr{Y}) \in [0, T] \times \mathbb{R}^4$,

(ii) Local Lipschitz continuity in $\mathscr{Y}$, uniformly in $t \in [0, T]$.

Proof. (i) Each component of $\mathscr{F}$ is composed of rational and polynomial expressions in the components of $\mathscr{Y}$, and does not explicitly depend on t. The only non-polynomial term is $\dfrac{rXV}{\kappa + V}$, which is continuous for all $V > -\kappa$. Since $\kappa > 0$ and we consider $V(t) \geq 0$ in biological models, the denominator never vanishes. Therefore, all component functions f_i of $\mathscr{F}$ are continuous, and thus $\mathscr{F}(t, \mathscr{Y})$ is jointly continuous in $(t, \mathscr{Y}) \in [0, T] \times \mathbb{R}^4$.

(ii) We compute the Jacobian matrix $D_{\mathscr{Y}} \mathscr{F}$ of partial derivatives with respect to $\mathscr{Y} = (X(t), Y(t), Z(t), V(t))^T$. Denoting the components of $\mathscr{F}$ by f_1, f_2, f_3, f_4. To clarify the computation, consider the first component

$$f_1(X, V) = \Lambda + \frac{rX(t)V(t)}{\kappa + V(t)} - \mu X(t)V(t) - \delta_1 X(t).$$

Taking the partial derivative of f_1 with respect to $V(t)$ gives

$$\frac{\partial f_1}{\partial V(t)} = rX(t)\frac{\partial}{\partial V(t)}\left(\frac{V(t)}{\kappa + V(t)}\right) - \mu X(t) = rX(t)\frac{\kappa}{(\kappa + V(t))^2} - \mu X(t),$$

which yields the corresponding Jacobian entry used in the analysis.

$$\frac{\partial f_1}{\partial X(t)} = \frac{rV(t)}{\kappa + V(t)} - \mu V(t) - \delta_1, \quad \frac{\partial f_1}{\partial V(t)} = \frac{rX(t)\kappa}{(\kappa + V(t))^2} - \mu X(t),$$

$$\frac{\partial f_2}{\partial X(t)} = \gamma \mu V(t), \quad \frac{\partial f_2}{\partial Y(t)} = -\delta_2, \quad \frac{\partial f_2}{\partial Z(t)} = \sigma, \quad \frac{\partial f_2}{\partial V(t)} = \gamma \mu X(t),$$

$$\frac{\partial f_3}{\partial X(t)} = (1-\gamma)\mu V(t), \quad \frac{\partial f_3}{\partial Z(t)} = -(\sigma + \delta_3), \quad \frac{\partial f_3}{\partial V(t)} = (1-\gamma)\mu X(t),$$

$$\frac{\partial f_4}{\partial Y(t)} = \xi, \quad \frac{\partial f_4}{\partial V(t)} = -\delta_4.$$

All partial derivatives are continuous functions of $\mathscr{Y}$, and therefore bounded on any compact subset $K \subset \mathbb{R}^4$. Thus, the Jacobian matrix $D_{\mathscr{Y}} \mathscr{F}$ is continuous and bounded on K, and by the Mean Value Theorem in $\mathbb{R}^4$, $\mathscr{F}$ is locally Lipschitz in $\mathscr{Y}$ on K. Since $\mathscr{F}$ is autonomous (i.e., does not depend on t), the local Lipschitz constant is uniform in $t \in [0, T]$.

Since the denominator $\kappa + V(t)$ is strictly positive for $V(t) \geq 0$, each component $f_i(t, Y)$ is continuously differentiable on the positive orthant. Although the function $\dfrac{rX(t)V(t)}{\kappa + V(t)}$ is not globally Lipschitz on $\mathbb{R}$, it is Lipschitz continuous on any bounded subset of the biologically feasible region $V(t) \geq 0$, which suffices for existence and uniqueness. $\square$

The Caputo fractional-order system is equivalent to the following Volterra-type integral equation:

$$\mathscr{Y}(t) = \mathscr{Y}_0 + \frac{1}{\Gamma(\theta)} \int_0^t (t-s)^{\theta-1} \mathscr{F}(s, \mathscr{Y}(s))\,ds,$$

where $\mathscr{Y}_0 \in \mathbb{R}^4$ is the initial condition, and $\mathscr{F}$ represents the right-hand side of the system.

Remark For $\theta \in (0, 1)$, the kernel $(t-s)^{\theta-1}$ is weakly singular but integrable: $\int_0^t (t-s)^{\theta-1}ds = t^\theta/\theta$. Consequently,

$$\frac{1}{\Gamma(\theta)} \int_0^t (t-s)^{\theta-1} F(s, Y(s)) \, ds,$$

is well defined for bounded F, and satisfies

$$\left\| \frac{1}{\Gamma(\theta)} \int_0^t (t-s)^{\theta-1} F(s, Y(s)) \, ds \right\| \leq \frac{t^\theta}{\Gamma(1+\theta)} \|F\|_{L^\infty(0, T)}.$$

Thus the Caputo integral operator maps $C([0, T])$ into itself and the Picard iteration is well posed. To prove existence and uniqueness of solutions, we employ the Picard successive approximation method.

Define the iteration sequence:

$$\mathscr{Y}_0(t) := \mathscr{Y}_0,$$

$$\mathscr{Y}_{n+1}(t) := \mathscr{Y}_0 + \frac{1}{\Gamma(\theta)} \int_0^t (t-s)^{\theta-1} \mathscr{F}(s, \mathscr{Y}_n(s)) \, ds.$$

To justify the assumption $\|F(t, Y)\| \leq M$, we note that $F(t, Y)$ is continuous in t and locally Lipschitz in Y. Therefore, for any finite time interval $[0, T]$ and for all solutions constrained within a bounded domain

$$D = \{(t, Y) \in [0, T] \times \mathbb{R}^4 : \|Y\| \leq R\},$$

the function F attains its maximum due to continuity. Hence, there exists a finite constant $M = \max_{(t, Y) \in D} \|F(t, Y)\|$ such that $\|F(t, Y)\| \leq M$ for all $(t, Y) \in D$. This local bound is sufficient to ensure that the Picard iteration sequence $\{Y_n(t)\}$ remains uniformly bounded on $[0, T]$.

We first establish uniform boundedness. Assume $\|\mathscr{F}(t, \mathscr{Y})\| \leq M$ for all $t \in [0, T]$ and $\|\mathscr{Y}\| \leq R$. The boundedness of F can be verified from its structure. Since all model variables $(X(t), Y(t), Z(t), V(t))$ are positive and uniformly bounded by Theorem 1(ii), and since each component of $F(t, Y)$ involves only polynomial and rational functions with denominators $\kappa + V(t)$ (which are always positive for $\kappa > 0$), every component $f_i(t, Y)$ is bounded on $[0, T]$. Therefore, there exists a finite constant $M > 0$ such that $\|F(t, Y)\| \leq M$ for all $(t, Y) \in [0, T] \times \mathbb{R}^4$. Then, for all n,

$$\|\mathscr{Y}_{n+1}(t)\| \leq \|\mathscr{Y}_0\| + \frac{MT^\theta}{\Gamma(1+\theta)} =: R',$$

which implies that the sequence $\{\mathscr{Y}_n\}$ is uniformly bounded on $[0, T]$. Here, $\|\cdot\|$ denotes the standard Euclidean norm in $\mathbb{R}^4$, and when applied to functions $y \in C([0, T]; \mathbb{R}^4)$, we use the uniform (supremum) norm:

$$\|y\| := \sup_{t \in [0, T]} \|y(t)\|_{\mathbb{R}^4}.$$

To show equicontinuity, let $0 \leq t_1 < t_2 \leq T$. Then:

$$\|\mathscr{Y}_{n+1}(t_2) - \mathscr{Y}_{n+1}(t_1)\| \leq \frac{M}{\Gamma(\theta)} \int_{t_1}^{t_2} (t_2 - s)^{\theta-1} ds = \frac{M}{\Gamma(\theta+1)} (t_2 - t_1)^{\theta} \to 0 \quad \text{as} \quad |t_2 - t_1| \to 0.$$

Thus, the sequence $\{\mathscr{Y}_n\}$ is equicontinuous on $[0, T]$. By the Arzelà-Ascoli theorem, there exists a uniformly convergent subsequence $\{\mathscr{Y}_{n_k}\}$ such that $\mathscr{Y}_{n_k} \to \mathscr{Y} \in C([0, T]; \mathbb{R}^4)$.

Finally, we show that the limit function $\mathscr{Y}(t)$ satisfies the integral equation. This follows from:

• the Lipschitz continuity of $\mathscr{F}(t, \mathscr{Y})$,

• the uniform convergence $\mathscr{Y}_n \to \mathscr{Y}$, and

• the Dominated Convergence Theorem applied to the sequence of integrals.

Therefore, $\mathscr{Y}(t)$ is a solution to the original fractional system. Uniqueness follows from a standard contraction mapping argument in the Banach space $C([0, T]; \mathbb{R}^4)$, completing the proof.

So, we have the following result:

Theorem 2 Let $\mathscr{F} : [0, T] \times \mathbb{R}^4 \to \mathbb{R}^4$ be continuous in t and locally Lipschitz in $\mathscr{Y}$. Then the Caputo fractional-order initial value problem:

$$^C D_t^{\theta} \mathscr{Y}(t) = \mathscr{F}(t, \mathscr{Y}(t)), \quad \mathscr{Y}(0) = \mathscr{Y}_0,$$

has at least one solution $\mathscr{Y} \in C([0, T]; \mathbb{R}^4)$, which is the uniform limit of a sequence of successive approximations.

Next, we show the uniqueness of the solution. Assume two solutions $y_1, y_2 \in \mathscr{X}$. Define the error function:

$$e(t) := \|y_1(t) - y_2(t)\|.$$

Using the integral form:

$$e(t) \leq \frac{1}{\Gamma(\theta)} \int_0^t (t - s)^{\theta-1} \|f(s, y_1(s)) - f(s, y_2(s))\| ds.$$

Assuming a Lipschitz constant L:

$$e(t) \leq \frac{L}{\Gamma(\theta)} \int_0^t (t - s)^{\theta-1} e(s) ds.$$

From the integral inequality:

$$e(t) \leq \frac{L}{\Gamma(\theta)} \int_0^t (t - s)^{\theta-1} e(s) ds,$$

we apply the fractional Grönwall inequality [30], which yields

$$e(t) \leq e(0) E_{\theta}(Lt^{\theta}),$$

where $E_\theta(\cdot)$ is the one-parameter Mittag-Leffler function. Because the two solutions share identical initial data, $e(0) = \|y_1(0) - y_2(0)\| = 0$. Therefore,

$$e(t) \leq 0 \times E_\theta(Lt^\theta) = 0,$$

which implies $e(t) = 0$ for all $t \in [0, T]$.

Theorem 3 Let $f : [0, T] \times \mathbb{R}^4 \to \mathbb{R}^4$ be continuous in t, locally Lipschitz in y, and bounded on bounded subsets of $\mathbb{R}^4$. Then the Caputo fractional-order initial value problem admits a unique local solution $y(t) \in C([0, T]; \mathbb{R}^4)$, which by Theorem 1(ii) (boundedness) extends to a unique global solution on $[0, T]$.

3.2 *Picard stability analysis of the caputo fractional-order HIV model*

We consider the Caputo fractional-order Initial Value Problem (IVP) derived from the HIV model:

$$^C D_t^\theta \mathbf{Y}(t) = \mathbf{F}(t, \mathbf{Y}(t)), \quad \mathbf{Y}(0) = \mathbf{Y}_0, \tag{4}$$

where $\mathbf{Y}(t) \in \mathbb{R}^4$, $\theta \in (0, 1]$, and $\mathbf{F} : [0, T] \times \mathbb{R}^4 \to \mathbb{R}^4$ is continuous in t and locally Lipschitz in $\mathbf{Y}$. The equivalent integral form using the Caputo derivative is:

$$\mathbf{Y}(t) = \mathbf{Y}_0 + \frac{1}{\Gamma(\theta)} \int_0^t (t-s)^{\theta-1} \mathbf{F}(s, \mathbf{Y}(s)) \, ds. \tag{5}$$

Define the iterative sequence $\{\mathbf{Y}_n(t)\}$:

$$\mathbf{Y}_0(t) := \mathbf{Y}_0,$$

$$\mathbf{Y}_{n+1}(t) := \mathbf{Y}_0 + \frac{1}{\Gamma(\theta)} \int_0^t (t-s)^{\theta-1} \mathbf{F}(s, \mathbf{Y}_n(s)) \, ds.$$

To analyze stability, we consider another sequence $\{\widetilde{\mathbf{Y}}_n(t)\}$ starting from perturbed initial value $\widetilde{\mathbf{Y}}_0$. Define the error function:

$$e_n(t) := \|\mathbf{Y}_n(t) - \widetilde{\mathbf{Y}}_n(t)\|. \tag{6}$$

Assuming $\mathbf{F}$ is Lipschitz continuous in $\mathbf{Y}$ with constant $L > 0$, we get:

$$e_{n+1}(t) = \|\mathbf{Y}_{n+1}(t) - \widetilde{\mathbf{Y}}_{n+1}(t)\|$$

$$= \left\| \mathbf{Y}_0 - \widetilde{\mathbf{Y}}_0 + \frac{1}{\Gamma(\theta)} \int_0^t (t-s)^{\theta-1} \left[\mathbf{F}(s, \mathbf{Y}_n(s)) - \mathbf{F}(s, \widetilde{\mathbf{Y}}_n(s)) \right] ds \right\|$$

$$\leq \|\mathbf{Y}_0 - \widetilde{\mathbf{Y}}_0\| + \frac{L}{\Gamma(\theta)} \int_0^t (t-s)^{\theta-1} e_n(s) ds.$$

The fractional Grönwall inequality states:

$$\text{If } e(t) \leq a + \frac{L}{\Gamma(\theta)} \int_0^t (t-s)^{\theta-1} e(s) ds, \text{ then } e(t) \leq a E_\theta(Lt^\theta). \tag{7}$$

Here, $E_\theta(z)$ denotes the Mittag-Leffler function, defined by

$$E_\theta(z) = \sum_{k=0}^{\infty} \frac{z^k}{\Gamma(\theta k + 1)}.$$

Applying the inequality with $a = \|\mathbf{Y}_0 - \widetilde{\mathbf{Y}}_0\|$ yields:

$$e_n(t) \leq \|\mathbf{Y}_0 - \widetilde{\mathbf{Y}}_0\| E_\theta(Lt^\theta), \quad \forall t \in [0, T]. \tag{8}$$

Remark The function $E_\theta(Lt^\theta)$ plays a role analogous to e^{Lt} in classical ODEs. For $0 < \theta < 1$, it grows subexponentially and remains bounded on any finite interval $[0, T]$. Hence, the estimate $e_n(t) \leq \|Y_0 - \tilde{Y}_0\| E_\theta(Lt^\theta)$ demonstrates Lipschitz (Picard) stability, that is, continuous dependence of the solution on the initial data, rather than asymptotic or exponential stability.

3.3 *Equilibria and threshold dynamics*

We now analyze the equilibria and stability properties of the fractional-order HIV model (3).
Equilibria and threshold. The infection-free equilibrium is

$$E_0 = \left(\frac{\Lambda}{\delta_1}, \, 0, \, 0, \, 0 \right).$$

An endemic equilibrium (X^*, Y^*, Z^*, V^*) satisfies

$$Y^* = \frac{\delta_4}{\xi} V^*, \quad Z^* = \frac{(1-\gamma)\mu X^*}{\sigma + \delta_3} V^*, \quad \mu X^* \left(\gamma + \frac{\sigma(1-\gamma)}{\sigma + \delta_3} \right) = \frac{\delta_2 \delta_4}{\xi}.$$

Let $b := \frac{\sigma + \gamma \delta_3}{\sigma + \delta_3}$. Then $X^* = \frac{\delta_2 \delta_4}{\xi \mu b}$ and (Y^*, Z^*, V^*) follow.
Linearizing the infected block at E_0 (or comparing X^* with X at E_0) yields the basic reproduction number

$$\mathscr{R}_0 = \frac{\mu \, \xi \, \Lambda}{\delta_1 \, \delta_2 \, \delta_4} \frac{\sigma + \gamma \delta_3}{\sigma + \delta_3}.$$

Theorem 4 (Threshold and local stability for $0 < \theta \le 1$) For the Caputo system (3) with $0 < \theta \le 1$, the infection-free equilibrium E_0 is locally asymptotically stable if $\mathscr{R}_0 < 1$ and unstable if $\mathscr{R}_0 > 1$. When $\mathscr{R}_0 > 1$, the endemic equilibrium above exists.

Proof sketch At E_0 the Jacobian decouples. The X-block has eigenvalue $-\delta_1 < 0$. The infected (Y, Z, V) block has all eigenvalues with $\Re\lambda < 0$ iff $\mathscr{R}_0 < 1$; otherwise one eigenvalue satisfies $\Re\lambda > 0$. For Caputo order $0 < \theta \le 1$, a linear equilibrium is locally asymptotically stable iff $|\arg(\lambda)| > \dfrac{\theta\pi}{2}$ for all eigenvalues λ. Negative real eigenvalues satisfy this for every $\theta \in (0, 1]$, proving the claim. $\qquad\square$

Role of θ The threshold $\mathscr{R}_0$ does not depend on θ. However, the Mittag-Leffler decay (growth) entails slower transient dynamics for smaller θ, reflecting memory effects typical of fractional-order models.

3.4 *Numerical solution via Lubich's convolution quadrature*

To numerically solve the Caputo fractional-order HIV model, we employ Lubich's convolution quadrature method, which is based on applying linear multistep methods to the Laplace transform of the Caputo derivative. This approach is well-suited for fractional differential equations and offers stability and accuracy under smoothness assumptions. We use the values of parameter given in Table 1 for numerical simulations.

Let $t_n = nh$, where $h = T/N$ is the uniform time step. The Caputo derivative is approximated by

$$^{C}D_t^{\theta} y(t_n) \approx \frac{1}{h^{\theta}} \sum_{j=0}^{n} \omega_j^{(\theta)} y_{n-j}.$$

The weights $\omega_j^{(\theta)}$ are obtained from the generating function $(1-\zeta)^{-\theta}$, which originates from the Grünwald-Letnikov definition of the fractional derivative. In the convolution quadrature framework, these weights are generalized through the Laplace transform of the chosen linear multistep method and thus yield a consistent discretization of the Caputo derivative when initial conditions are imposed. For the backward Euler method, the generating function is:

$$^{C}D_t^{\theta} y(t_n) \approx \frac{1}{h^{\theta}} \sum_{j=0}^{n} \omega_j^{(\theta)} y_{n-j}, \quad \sum_{j=0}^{\infty} \omega_j^{(\theta)} \zeta^j = \left(\delta(\zeta)\right)^{-\theta}, \quad \delta(\zeta) = 1 - \zeta.$$

Let $\mathbf{y}(t_n) = \begin{bmatrix} X(t_n) & Y(t_n) & Z(t_n) & V(t_n) \end{bmatrix}^{\top}$. The nonlinear right-hand side of the HIV model becomes:

$$\mathbf{F}(t_n, \mathbf{y}(t_n)) = \begin{bmatrix} \Lambda + \dfrac{rX(t_n)V(t_n)}{\kappa + V(t_n)} - \mu X(t_n)V(t_n) - \delta_1 X(t_n) \\ \gamma\mu X(t_n)V(t_n) + \sigma Z(t_n) - \delta_2 Y(t_n) \\ (1 - \gamma)\mu X(t_n)V(t_n) - \sigma Z(t_n) - \delta_3 Z(t_n) \\ \xi Y(t_n) - \delta_4 V(t_n) \end{bmatrix}.$$

Lubich's method leads to the discrete form:

$$\frac{1}{h^{\theta}} \sum_{j=0}^{n} \omega_j^{(\theta)} \mathbf{y}_{n-j} = \mathbf{F}(t_n, \mathbf{y}_n),$$

which is a nonlinear system for $\mathbf{y}_n$. Rearranging yields the fixed-point iteration:

$$\mathbf{y}_n = \frac{h^\theta}{\omega_0^{(\theta)}} \left(\mathbf{F}(t_n, \mathbf{y}_n) - \sum_{j=1}^{n} \omega_j^{(\theta)} \mathbf{y}_{n-j} \right).$$

This is solved iteratively using:

$$\mathbf{y}_n^{(k+1)} = \frac{h^\theta}{\omega_0^{(\theta)}} \left(\mathbf{F}(t_n, \mathbf{y}_n^{(k)}) - \sum_{j=1}^{n} \omega_j^{(\theta)} \mathbf{y}_{n-j} \right),$$

starting from $\mathbf{y}_n^{(0)} = \mathbf{y}_{n-1}$. The iteration is terminated when:

$$\left\| \mathbf{y}_n^{(k+1)} - \mathbf{y}_n^{(k)} \right\| < \varepsilon.$$

Remark At each time level t_n, the implicit relation for y_n is solved using the fixed-point iteration

$$y_n^{(k+1)} = \frac{h^\theta}{\omega_0^{(\theta)}} \left(F\left(t_n, y_n^{(k)}\right) - \sum_{j=1}^{n} \omega_j^{(\theta)} y_{n-j} \right), \qquad k = 0, 1, 2, \ldots,$$

with initial guess $y_n^{(0)} = y_{n-1}$. Since F is Lipschitz continuous in y with constant L, the iteration map satisfies

$$\| \Phi(y) - \Phi(\tilde{y}) \| \leq \frac{h^\theta L}{|\omega_0^{(\theta)}|} \| y - \tilde{y} \|.$$

Hence the iteration converges whenever $\dfrac{h^\theta L}{|\omega_0^{(\theta)}|} < 1$ (for the backward Euler convolution quadrature, $\omega_0^{(\theta)} = 1$).
Under this standard stepsize restriction, convergence is guaranteed independently of the initial guess, and the choice $y_n^{(0)} = y_{n-1}$ is justified because the exact solution is continuous in time.

Theorem 5 [28] Let $f \in C^k([0, T])$, and consider the Caputo initial value problem:

$$^C D_t^\theta y(t) = f(t), \quad y(0) = y_0, \quad 0 < \theta < 1.$$

If a k-step A-stable linear multistep method is used to generate the convolution weights, then:
(i) The method converges with order $\mathcal{O}(h^k)$:

$$\| y(t_n) - y_n \| \leq Ch^k, \quad \text{for } 0 \leq t_n \leq T.$$

(ii) The method is stable under perturbations in data and initial conditions.

Since the discrete formula is implicit in y_n, we compute y_n iteratively using a fixed-point procedure. Because $F(t, Y)$ is locally Lipschitz, the iteration converges for sufficiently small step size h, guaranteeing a unique y_n at each step.

Remark 4 Although the theorem in [28] was proved for the linear Caputo equation ${}^C D_t^{\theta} y = f(t)$, the same reasoning extends to nonlinear systems ${}^C D_t^{\theta} Y = F(t, Y)$ under the usual Lipschitz and boundedness conditions on F. The proof uses the equivalent Volterra integral form and Picard iteration, which are valid for both linear and nonlinear F.

Table 1. Model parameters and initial conditions used in all simulations (baseline and ART cases)

Parameter	Description	Value	Units	Source
Λ	Recruitment rate of uninfected CD4$^+$ T cells	10	cells/mm^3/day	[31]
r	Maximum clonal growth rate of CD4$^+$ T cells	0.01	day^{-1}	[32]
κ	Half-saturation constant for T cell proliferation	300	virions/mL	[32]
μ	Infection rate of uninfected CD4$^+$ T cells by virus	0.00387	mL/(cell $\cdot$ day)	[33]
γ	Fraction of infected CD4$^+$ T cells that become active	0.97	–	[33]
σ	Activation rate of latently infected cells	0.0003	day^{-1}	[34]
ξ	Production rate of virions by infected cells	0.537	virions/(cell $\cdot$ day)	[34]
δ_1	Death rate of uninfected CD4$^+$ T cells	0.01	day^{-1}	[34]
δ_2	Death rate of actively infected CD4$^+$ T cells	0.28	day^{-1}	[34]
δ_3	Death rate of latently infected CD4$^+$ T cells	0.05	day^{-1}	[34]
δ_4	Clearance rate of free virions	2.39	day^{-1}	[34]
t_{ART}	Time of ART initiation	5	days	Assumed
ε_{μ}	ART efficacy in blocking infection	0.8	–	Assumed
ε_{ξ}	ART efficacy in reducing viral production	0.7	–	Assumed
X_0	Initial uninfected CD4$^+$ T cells	1,000	cells/mm^3	Assumed
Y_0	Initial infected CD4$^+$ T cells	270	cells/mm^3	Assumed
Z_0	Initial latently infected CD4$^+$ T cells	382	cells/mm^3	Assumed
V_0	Initial viral load	11,147	virions/mL	Assumed

Discussion: To assess the numerical accuracy of the Lubich convolution quadrature used in the fractional HIV simulations, we tested it on the linear model ${}^C D_t^{\theta} y(t) = -y(t)$, whose analytical solution is $y(t) = E_{\theta}(-t^{\theta})$. The estimated order of convergence p quantifies how rapidly the numerical error decays when the time step h is reduced, where a value $p = 1$ corresponds to first-order accuracy. As shown in Figure 1, the Backward Euler-Convolution Quadrature (BE-CQ) method reproduces the expected first-order convergence for $\theta = 0.9$ and $\theta = 1.0$, with a slight degradation for $\theta = 0.8$ due to the increased nonlocality of the Caputo derivative. This validation demonstrates that the time discretization employed in the HIV model is both accurate and stable for the range of fractional orders considered. Table 2 shows the numerical values of the accuracy.

Table 2. Global error $e(h)$ and estimated convergence order of the proposed approach for ${}^C D_t^{\theta} y = -y$, $y(0) = 1$, at $T = 1$

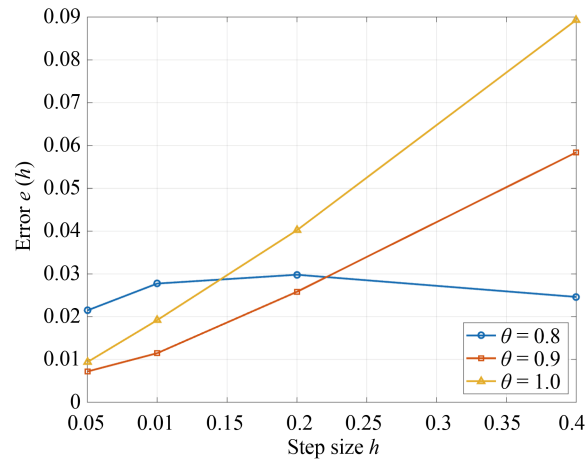| θ	Step size h				Estimated order
	0.4	0.2	0.1	0.05	
0.8	0.0246	0.0298	0.0277	0.0215	≈ 0.07
0.9	0.0584	0.0258	0.0115	0.0072	≈ 1.01
1.0	0.0893	0.0402	0.0192	0.0094	≈ 1.08

Figure 1. Order-of-accuracy verification of the BE-CQ scheme applied to the scalar test equation $^{C}D_t^{\theta} y(t) = -y(t)$, $y(0) = 1$. The global error $e(h) = \max_t |y_h(t) - y(t)|$ is plotted against the step size h in a log-log scale for fractional orders $\theta = 0.8, 0.9, 1.0$. The estimated convergence orders, computed as $p = \log(e(h_1)/e(h_2))/\log(h_1/h_2)$, are approximately $p \approx 0.07$, 1.01, and 1.08 for $\theta = 0.8$, 0.9, and 1.0, respectively. The results confirm that the BE-CQ scheme achieves nearly first-order accuracy for smooth problems, consistent with theoretical predictions, while the slight loss of accuracy for smaller θ reflects stronger memory effects of the fractional derivative

4. Graphical analysis

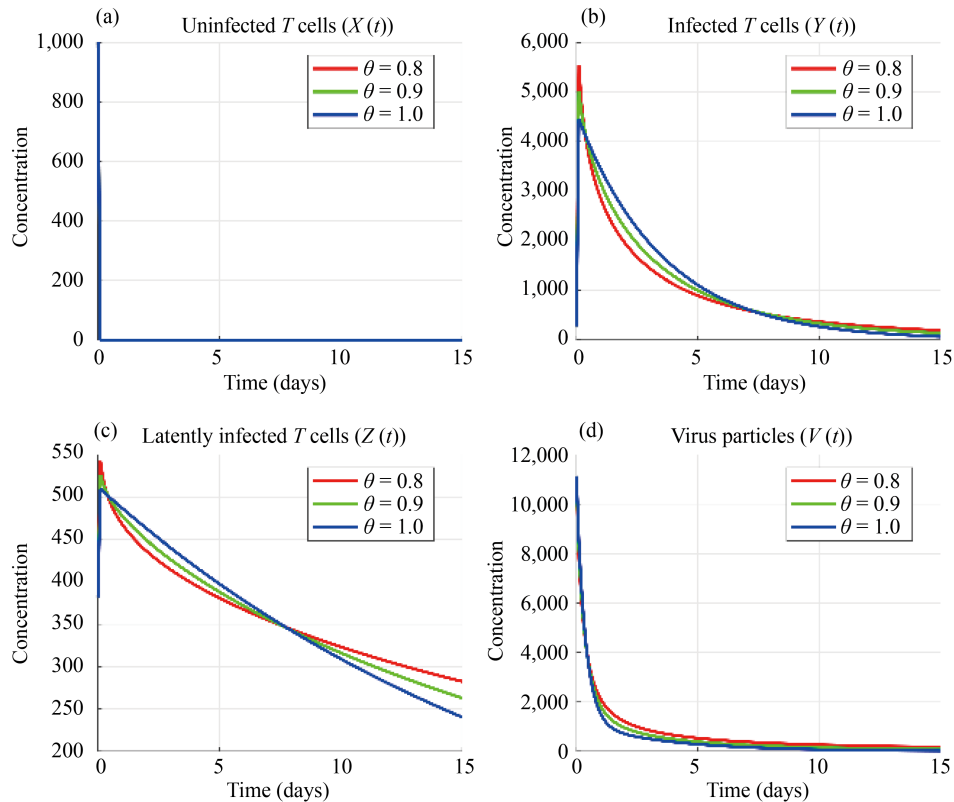We use the values of parameter given in Table 1 for numerical simulations.

Figure 2. Simulations of uninfected, infected, and latently infected T cells, as well as virus particles over time, for different fractional orders ($\theta = 0.8$, 0.9, 1.0) in the absence of ART intervention

Figure 2 presents simulations of the HIV model under different fractional orders $\theta \in \{0.8, 0.9, 1.0\}$ without ART. The Caputo derivative with order $\theta \in (0, 1]$ introduces a memory effect into the system, which slows or accelerates the response depending on the value of θ. Figure 2a displays simulations of uninfected T cells $X(t)$. We observe that as θ increases, $X(t)$ recovers more rapidly. At $\theta = 0.8$, recovery is sluggish due to stronger memory effects, while at $\theta = 1.0$, the immune response is more immediate and $X(t)$ increases faster. Figure 2b presents the dynamics of infected T cells $Y(t)$. It is observed that a higher θ results in a lower peak and faster decline. Lower θ values slow the clearance of infected cells due to memory effects, whereas for $\theta = 1.0$, the clearance is more efficient. Figure 2c provides graphical results of latently infected T cells $Z(t)$. We note that $Z(t)$ stabilizes at a higher level for smaller θ. Stronger memory ($\theta = 0.8$) maintains a larger latent reservoir. As θ increases, $Z(t)$ decreases over time. Figure 2d demonstrates the concentration of virus particles $V(t)$. We observe that peak viral load is highest for $\theta = 0.8$ and lowest for $\theta = 1.0$. At higher θ, viral clearance is faster and more effective. Overall, lower θ values imply stronger memory effects, leading to slower system dynamics and delayed recovery. The classical model ($\theta = 1$) shows a faster immune response and better viral control.
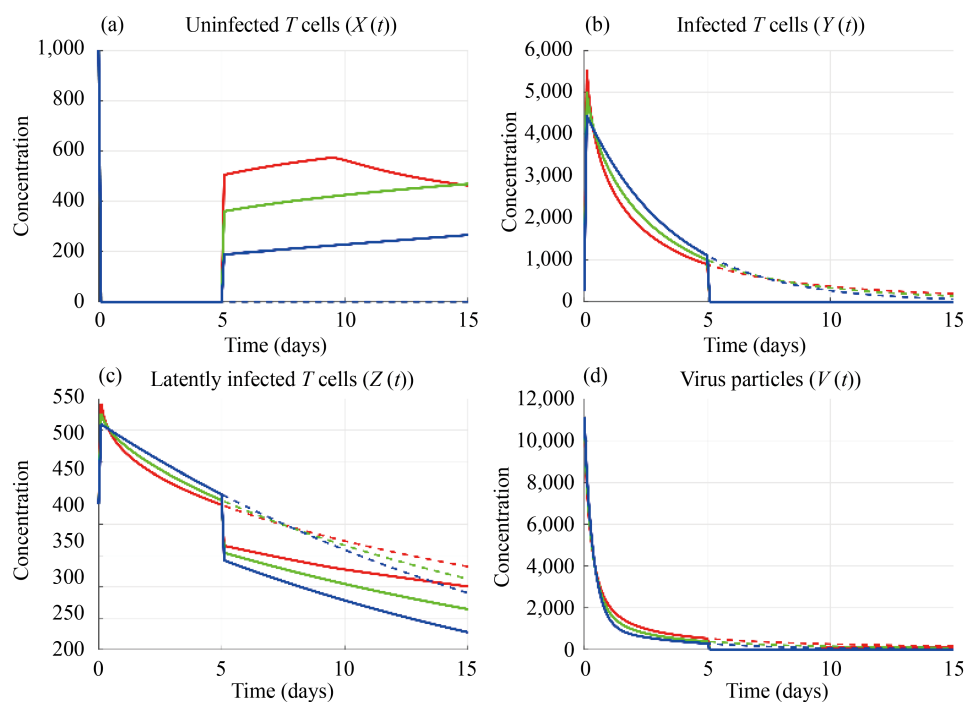

Figure 3. Comparison of immune and viral dynamics with and without ART for various fractional orders. Treatment begins at $t_{\text{ART}} = 5$ days with $\varepsilon_\mu = 0.8$ and $\varepsilon_\xi = 0.7$, corresponding to 80% and 70% reductions in infection and viral production, respectively

Figure 3 compares the dynamics under ART and no ART for each $\theta \in \{0.8, 0.9, 1.0\}$. ART is simulated by modifying parameters to reflect treatment, such as reducing the infection rate (μ), increasing viral clearance (δ_4), or suppressing viral production (ξ). As shown in Figure 3a, ART leads to faster and more complete recovery of $X(t)$. ART prevents infection of new T cells, and its effectiveness is more pronounced at $\theta = 1.0$. In Figure 3b, it is observed that ART dramatically reduces $Y(t)$ for all θ. ART effectively limits the transition from X to Y and reactivation from Z. Larger θ accelerates this suppression. Figure 3c shows that ART limits the latent pool $Z(t)$. ART may inhibit entry into latency or promote decay/reactivation, thereby reducing $Z(t)$ over time. The effectiveness of ART improves with increasing θ. In Figure 3d, we observe that ART significantly reduces the viral load. ART suppresses viral production and/or enhances viral clearance. Viral suppression is fastest for $\theta = 1.0$.

Overall, ART is effective across all values of θ, but the speed of response and level of suppression vary. As θ increases, ART becomes more effective due to faster system dynamics and reduced memory drag. Table 3 provides a summary of the graphical results.

Table 3. Effect of varying fractional order θ on immune dynamics and ART effectiveness. Lower values of θ reflect stronger memory effects, resulting in slower immune response and reduced ART efficiency

Fractional order θ	Immune/Viral dynamics	ART effectiveness
$\theta = 0.8$	Slow, memory-dominant	Slower response
$\theta = 0.9$	Intermediate dynamics	Moderate response
$\theta = 1.0$	Classical ODE	Fastest response

Effect of infection rate μ:

In the absence of ART shown in Figure 4, increasing μ leads to higher peaks and slower decay in the trajectories of infected cells $Y(t)$, latent cells $Z(t)$, and virus particles $V(t)$. This indicates stronger viral propagation and a more persistent latent reservoir. However, with ART intervention displayed in Figure 5, all compartments drop sharply after treatment initiation at $t = 5$, and the trajectories for different μ values converge. This suggests that ART effectively suppresses infection progression regardless of the initial infection rate.
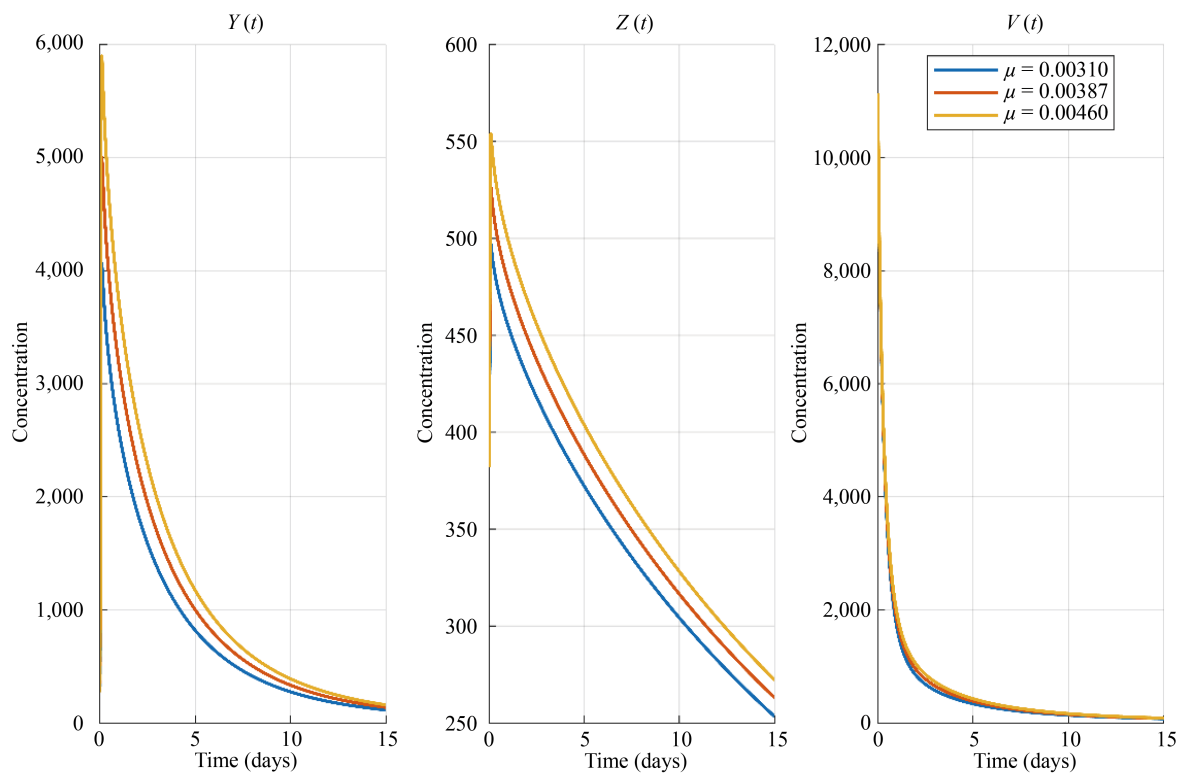

Figure 4. Influence of the parameter μ on $Y(t)$, $Z(t)$ and $V(t)$ with $\theta = 0.9$
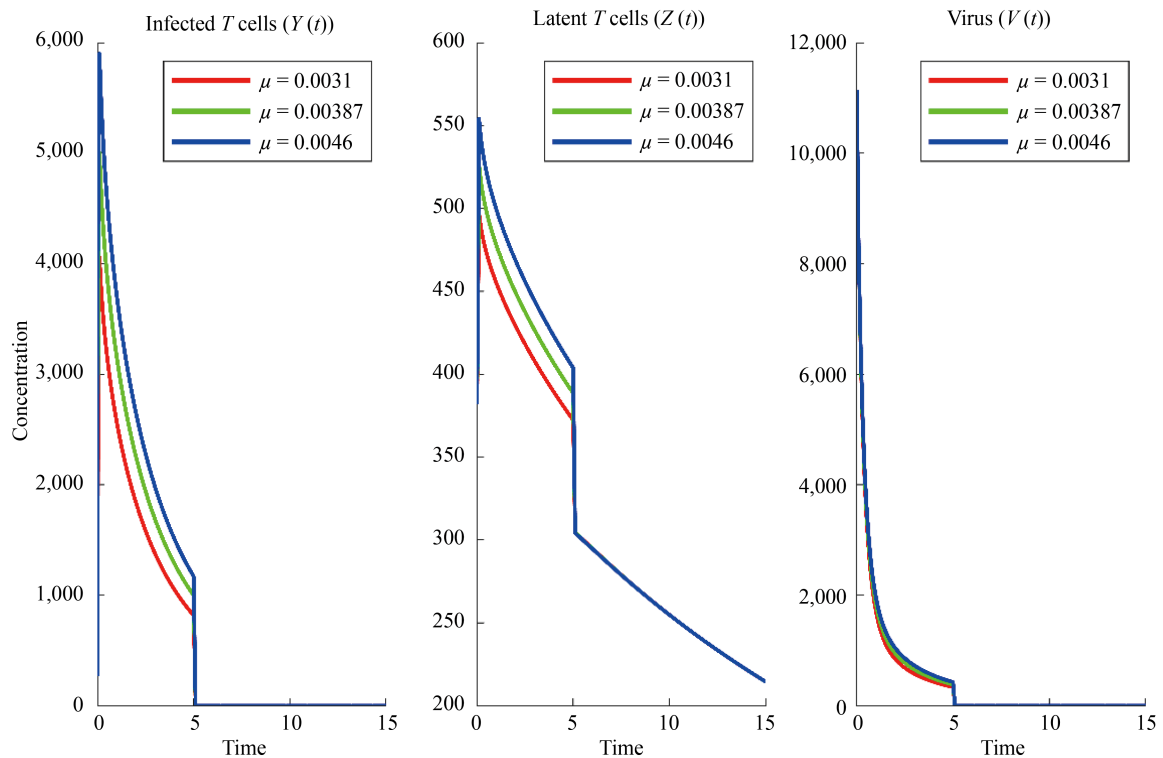
Figure 5. Influence of the parameter μ on $Y(t)$, $Z(t)$ and $V(t)$ with ART and $\theta = 0.9$. Treatment begins at $t_{\text{ART}} = 5$ days with $\varepsilon_\mu = 0.8$ and $\varepsilon_\xi = 0.7$, corresponding to 80% and 70% reductions in infection and viral production, respectively
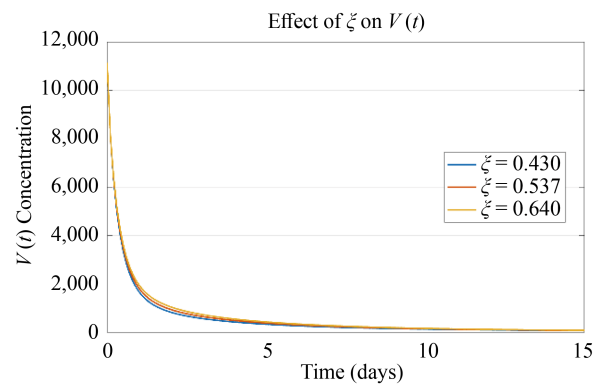

Figure 6. Influence of the parameter ξ on $V(t)$ with $\theta = 0.9$

Effect of viral production rate ξ:

Figure 6 shows that higher values of ξ modestly increase the viral load $V(t)$ prior to treatment. After ART is introduced as depicted in Figure 7, all viral load trajectories collapse regardless of the initial ξ, demonstrating that ART's suppression of viral production dominates baseline variation in this parameter.
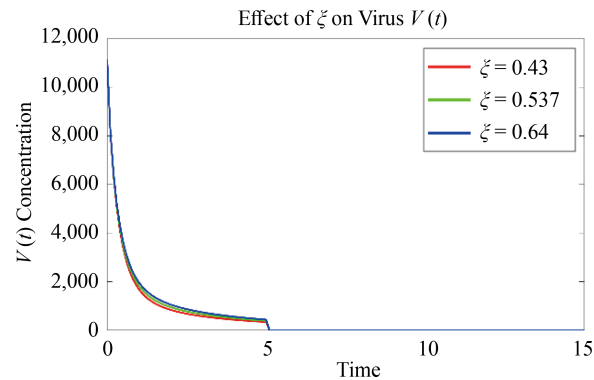
Figure 7. Influence of the parameter ξ on $V(t)$ with ART and $\theta = 0.9$. Treatment begins at $t_{ART} = 5$ days with $\varepsilon_\mu = 0.8$ and $\varepsilon_\xi = 0.7$, corresponding to 80% and 70% reductions in infection and viral production, respectively

Effect of infected cell clearance rate δ_2:

In Figure 8, without ART, increasing δ_2 accelerates the decline of infected T-cells $Y(t)$ and slightly reduces $V(t)$. Under ART, this effect becomes more pronounced; higher δ_2 leads to a steeper decline in both $Y(t)$ and $V(t)$ after treatment, initiation as shown in Figure 9. This highlights the importance of infected cell clearance in enhancing ART efficacy.

These comparisons illustrate that while parameter variability significantly shapes the pre-ART dynamics, the initiation of ART strongly dominates the system behavior, mitigating the long-term influence of these parameters.

Biological Interpretation.

The fractional-order model highlights how memory effects influence HIV progression. Lower values of the fractional order θ correspond to stronger immune memory, leading to slower recovery, prolonged viral load $V(t)$, and sustained latent infection $Z(t)$. Simulation results show that ART is more effective at higher θ values, suggesting earlier treatment may yield better outcomes. These insights can support the timing and design of ART strategies, offering a more realistic approach to managing chronic HIV infection.

The fractional parameter θ plays a critical role in modeling the immune system's memory and chronicity in real-world HIV infection. In clinical terms, lower values of θ (e.g., $\theta = 0.8$) can represent individuals with a weakened or delayed immune response-such as late-stage HIV patients or those co-infected with immunosuppressive diseases. These patients often exhibit prolonged viremia, slower CD4$^+$ T cell recovery, and persistent latent reservoirs, all of which are consistent with the slower system dynamics captured by lower θ values in our model.

Conversely, higher values of θ (e.g., $\theta = 0.9$ or 1.0) may correspond to individuals who initiate ART early, maintain good treatment adherence, or have a relatively robust immune system. These cases show faster viral suppression and immune reconstitution, behaviors mirrored in the model dynamics when θ approaches 1 (the classical ODE case). Thus, varying θ offers a way to simulate and analyze clinical heterogeneity in immune memory and response time, thereby enhancing the model's relevance to patient-specific treatment outcomes.

Model Limitations.

The present fractional-order HIV model considers a single-host system and does not include explicit Pharmacokinetic/ Pharmacodynamic (PK/PD) interactions, drug resistance evolution, or stochastic effects such as measurement noise. The latency stage is modeled as a lumped compartment, and immune response mechanisms are not explicitly represented. Future extensions could incorporate multi-drug ART regimens, PK-modulated efficacy, or immune feedback to more accurately reflect clinical dynamics. Such extensions would allow for quantitative exploration of how fractional memory interacts with treatment heterogeneity.
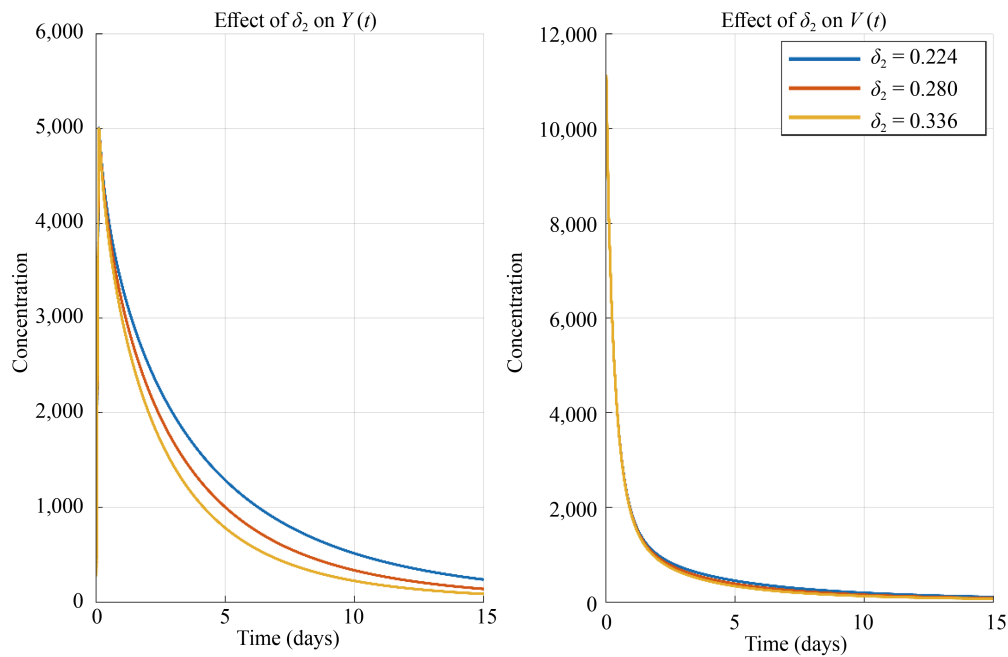
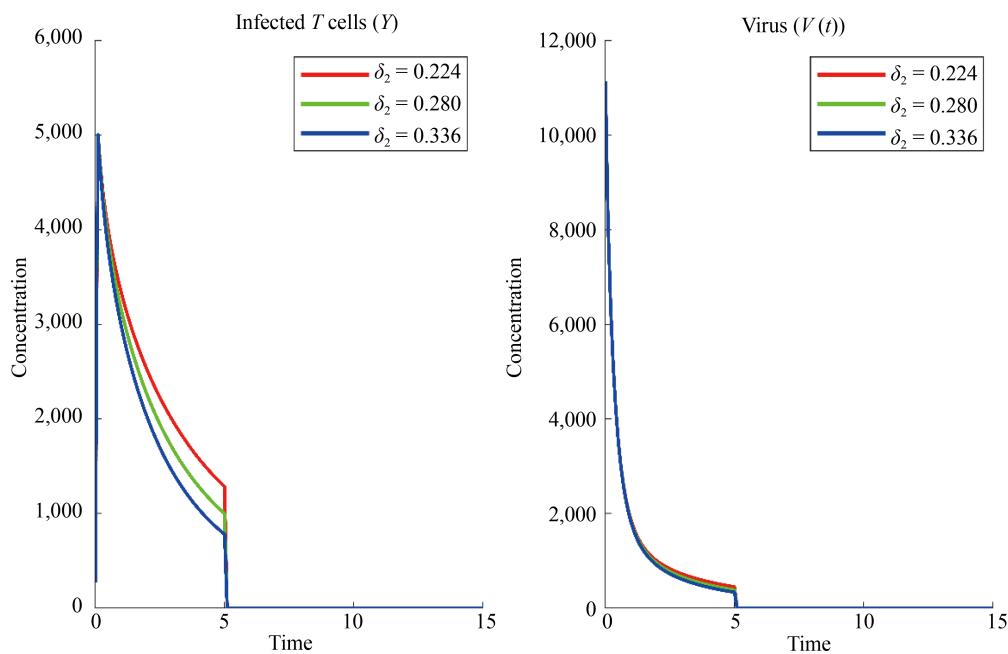**Figure 8.** Influence of the parameter μ on $Y(t)$, $Z(t)$ and $V(t)$ with $\theta = 0.9$

Figure 9. Influence of the parameter μ on $Y(t)$, $Z(t)$ and $V(t)$ with ART and $\theta = 0.9$. Treatment begins at $t_{\mathrm{ART}} = 5$ days with $\varepsilon_\mu = 0.8$ and $\varepsilon_\xi = 0.7$, corresponding to 80% and 70% reductions in infection and viral production, respectively

5. Summary

This paper presents a comprehensive theoretical and numerical analysis of a Caputo fractional-order HIV model with and without ART intervention. By introducing memory effects into the model dynamics, we capture key features of

chronic infection behavior that classical integer-order models overlook. We analytically proved essential mathematical properties of the model positivity, boundedness, existence, and uniqueness using fixed-point theorems and properties of Caputo derivatives.

A Picard-based stability analysis demonstrated that small perturbations in initial data yield proportionally small deviations in model output, reinforcing solution reliability. We applied Lubich's convolution quadrature method to numerically simulate the model with high stability and accuracy. Simulation results reveal that lower fractional orders lead to slower immune responses and viral clearance due to stronger memory effects, whereas the classical case $\theta = 1$ corresponds to faster system dynamics. The inclusion of ART significantly enhances recovery and viral suppression across all orders, with greater efficacy at higher fractional orders.

Data availability statement

All data are fully available in the manuscript without restriction.

Acknowledgment

Conflicts of interest

The authors declare no conflict of interest.

References

[1] Xu C, Muhammad F, Aamir S, Kottakkaran SN. Modeling and Ulam-Hyers stability analysis of oleic acid epoxidation by using a fractional-order kinetic model. *Mathematical Methods in the Applied Sciences*. 2025; 48(3): 3726-3747.

[2] Xu C, Muhammad F, Aamir S. Analysis and chaotic behavior of a fish farming model with singular and non-singular kernel. *International Journal of Biomathematics*. 2025; 18(3): 2350105.

[3] Xua C, Maoxin L, Muhammad F, Aamir S. Hydrogenolysis of glycerol by heterogeneous catalysis: a fractional order kinetic model with analysis. *Communications in Mathematical and in Computer Chemistry*. 2024; 91(3): 635-664.

[4] Iskakova K, Mohammad MA, Shabir A, Sayed S, Ali A, Gülnur Y. Dynamical study of a novel 4D hyperchaotic system: An integer and fractional order analysis. *Mathematics and Computers in Simulation*. 2023; 208: 219-245.

[5] Manivel M, Venkatesh A, Shyamsunder K. A comprehensive study of monkeypox disease through fractional mathematical modeling. *Mathematical Modelling and Numerical Simulation with Applications*. 2025; 5(1): 65-96.

[6] Liu X, Mati R, Saeed A, Dumitru B, Yasir NA. A new fractional infectious disease model under the non-singular Mittag-Leffler derivative. *Waves in Random and Complex Media*. 2025; 35(1): 1617-1643.

[7] Fauzi IS, Nuning N, Ade Maya S, Imaniah BW, Delsi T, Purnama MS, et al. Assessing the impact of booster vaccination on diphtheria transmission: Mathematical modeling and risk zone mapping. *Infectious Disease Modelling*. 2024; 9(1): 245-262.

[8] Zhao Y, Xu C, Xu Y, Lin J, Pang YC, Liu ZX, et al. Mathematical exploration on control of bifurcation for a 3D predator-prey model with delay. *AIMS Mathematics*. 2024; 9(11): 29883-29915.

[9] Xu ZB, Zhang HM, Yang DY, Wei DQ, Jacques D, Zeng QC. The Mathematical modeling of the host-virus Interaction in dengue virus infection: a quantitative study. *Viruses*. 2024; 16(2): 216.

[10] Shabir A, Ullah A, Partohaghighi M, Saifullah S, Akgül A, Jarad F. Oscillatory and complex behaviour of Caputo-Fabrizio fractional order HIV-1 infection model. *AIMS Mathematics*. 2022; 7(3): 4778-4792.

[11] Liu X, Shabir A, Aman U, Sayed S, Ali A, Haidong Q. Bifurcations, stability analysis and complex dynamics of Caputo fractal-fractional cancer model. *Chaos, Solitons & Fractals*. 2022; 159: 112113.

[12] Alraqad T, Almalahi MA, Mohammed N, Alahmade A, Aldwoah KA, Saber H. Modeling ebola dynamics with a Φ-piecewise hybrid fractional derivative approach. *Fractal and Fractional*. 2024; 8(10): 596.

[13] Aldwoah KA, Almalahi MA, Hleili M. Analytical study of a modified-ABC fractional order breast cancer model. *Journal of Applied Mathematics and Computing*. 2024; 70: 3685-3716.

[14] Saber H, Almalahi MA, Albala H, Aldwoah K, Alsulami A, Shah K, et al. Investigating a nonlinear fractional evolution control model using W-piecewise hybrid derivatives: an application of a breast cancer model. *Fractal and Fractional*. 2024; 8(12): 735.

[15] Hamza AE, Osman O, Ali A, Alsulami A, Aldwoah K, Mustafa A, et al. Fractal-fractional-order modeling of liver fibrosis disease and its mathematical results with subinterval transitions. *Fractal and Fractional*. 2024; 8(11): 638.

[16] Bhangale N, Krunal BK, Gómez-Aguilar JF. Fractional viscoelastic models with Caputo generalized fractional derivative. *Mathematical Methods in the Applied Sciences*. 2023; 46(7): 7835-7846.

[17] Kassimi S, Moussa H, Sabiki H. Enhancing image denoising: A novel non-local anisotropic diffusion framework based on Caputo derivatives and Gaussian convolution for the Perona-Malik model. *Signal Processing*. 2024; 222: 109521.

[18] Salama, FM, Faisal F. On numerical solution of two-dimensional variable-order fractional diffusion equation arising in transport phenomena. *AIMS Mathematics*. 2024; 9(1): 340-370.

[19] Naik PA, Naveen S, Parthiban V, Sania Q, Marwan A, Mehmet S. Advancing lotka-volterra system simulation with variable fractional order caputo derivative for enhanced dynamic analysis. *Journal of Applied Analysis & Computation*. 2025; 15(2): 1002-1019.

[20] Silverberg MJ, Chun C, Wendy AL, Lanfang X, Michael AH, Daniel K, et al. HIV infection, immunodeficiency, viral replication, and the risk of cancer. *Cancer Epidemiology, Biomarkers & Prevention*. 2011; 20(12): 2551-2559.

[21] Dorratoltaj N, Ryan NB, Stanca MC, Stephen GE, Kaja MA. Multi-scale immunoepidemiological modeling of within-host and between-host HIV dynamics: systematic review of mathematical models. *PeerJ*. 2017; 5: e3877.

[22] Deng Q, Guo T, Qiu ZP, Chen YM. A mathematical model for HIV dynamics with multiple infections: implications for immune escape. *Journal of Mathematical Biology*. 2024; 89(1): 6.

[23] Pathak R, Tarun K, Rakesh K. Mathematical model for the transmission dynamics of HIV-scrub typhus co-infection. *Modeling Earth Systems and Environment*. 2025; 11(2): 103.

[24] Fatmawati EMS, Mohammad IU. A fractional-order model for HIV dynamics in a two-sex population. *International Journal of Mathematics and Mathematical Sciences*. 2018; 1: 6801475.

[25] Cai J, Zhang J, Wang K, Dai ZX, Hu ZL, Dong YP, et al. Evaluating the long-term effects of combination antiretroviral therapy of HIV infection: a modeling study. *Journal of Mathematical Biology*. 2024; 90(4): 1-32.

[26] Ionescu C, Lopes A, Dana Copot JA, Jason HTB. The role of fractional calculus in modeling biological phenomena: A review. *Communications in Nonlinear Science and Numerical Simulation*. 2017; 51: 141-159.

[27] Magin RL. Fractional calculus models of complex dynamics in biological tissues. *Computers & Mathematics with Applications*. 2010; 59(5): 1586-1593.

[28] Lubich C. A stability analysis of convolution quadraturea for Abel-Volterra integral equations. *IMA Journal of Numerical Analysis*. 1986; 6(1): 87-101.

[29] Saifullah S, Amir A, Zareen AK. Analysis of nonlinear time-fractional Klein-Gordon equation with power law kernel. *AIMS Mathematics*. 2022; 7(4): 5275-5290.

[30] Denton Z, Aghalaya SV. Fractional integral inequalities and applications. *Computers & Mathematics with Applications*. 2010; 59(3): 1087-1094.

[31] Perelson AS, Kirschner DE, De Boer R. Dynamics of HIV infection of $CD4^+$ T cells. *Bulletin of Mathematical Biology*. 1993; 55: 3-36.

[32] Pankavich S, Loudon J, Hellmich EC. Bistability in HIV models with homeostatic proliferation of $CD4^+$ T cells. *Mathematical Biosciences and Engineering*. 2020; 17(2): 1678-1699.

[33] Hadjiandreou MM, Conejeros S, Georgiou DP. A HIV infection model with latently infected cells and viral loss in latent stage. *Mathematical Biosciences and Engineering*. 2007; 4(2): 287-300.

[34] Dong Y, Ma Z. Global stability of an HIV infection model with latent infection and treatment. *Mathematical Biosciences and Engineering*. 2012; 9(4): 885-900.